ICHEP'98 #201
Submitted to Pa 10
Pl 12

DELPHI 98-66 CONF 134
22 June, 1998

# Search for charginos, neutralinos and gravitinos at $\sqrt{s} = 183$ GeV

Preliminary

DELPHI Collaboration

**P.Andersson** [1], **I.Gil** [2], **A.Lipniacka** [1], **S.Navas** [2], **P.Rebecchi** [3], **K.Hultqvist** [1]

**Abstract**

An update of the searches for charginos and neutralinos is presented, based on a data sample corresponding to the 53.9 pb$^{-1}$ recorded by the DELPHI detector in 1997, at a centre-of-mass energy of 183 GeV. No evidence of a signal was found. For a sneutrino with mass above 300 GeV/$c^2$ and a mass difference between the chargino and the lightest neutralino above 10 GeV/$c^2$ the lower limit at 95 % confidence level on the chargino mass ranges from 89.4 GeV/$c^2$ to 90.8 GeV/$c^2$, depending on the mixing parameters. This limit decreases for lower mass differences ($\sim$ 5 GeV/$c^2$) to 88.8 GeV/$c^2$. In this case a sneutrino of $m_{\tilde{\nu}}$ >41 GeV/$c^2$ is assumed. The ($\mu$,M$_2$) domain excluded combining the neutralino and chargino searches implies a limit on the mass of the lightest neutralino which, for a heavy sneutrino, is constrained to be above 29.1 GeV/$c^2$ for $\tan\beta \geq 1$. The search of charginos has also been extended to the case where the lightest neutralino is unstable and decays into a photon and a gravitino. The quoted mass limits in this case are 90.5 GeV/$c^2$ for large mass differences between the chargino and the NLSP, and 90.6 GeV/$c^2$ for lower mass differences ($\sim$ 1 GeV/$c^2$).

Paper submitted to the ICHEP'98 Conference
Vancouver, July 22-29

[1] Fysikum, Stockholm University, Box 6730, S-113 85 Stockholm, Sweden
[2] IFIC, Valencia-CSIC and DFAMN, U. de Valencia, E-46100 Burjassot (Valencia), Spain
[3] CERN, CH-1211 Geneva 23, Switzerland

# 1 Introduction

In 1997, the LEP centre-of-mass energy reached 183 GeV, and the DELPHI experiment collected an integrated luminosity of 53.9 $\mathrm{pb}^{-1}$. These data have been analysed to search for the supersymmetric partners of Higgs and gauge bosons, the charginos, neutralinos and gravitinos, predicted by supersymmetric (SUSY) models [1].

This paper is an update of the results described in [2], which contains a detailed description of the analysis. The methods used to search for charginos and neutralinos presented in [2] have remained almost unchanged and only the differences from the previous analysis are described here. A description of the parts of the DELPHI detector relevant to the present paper can be found in [2], while the complete descriptions are given in [17].

The conservation of R-parity, implying a stable lightest supersymmetric particle (LSP), is assumed. As in the previous paper both the cases where either the lightest neutralino ($\tilde{\chi}_1^0$) or the gravitino ($\tilde{\mathrm{G}}$) is the LSP are considered. In the former case, events are characterised by missing energy carried by the escaping neutralinos, while in the latter case the decay $\tilde{\chi}_1^0 \to \tilde{\mathrm{G}}\gamma$ is possible [3, 4, 5]. If the gravitino is sufficiently light (with a mass below about 10 $\mathrm{eV}/c^2$ [5]), this decay takes place within the detector. As gravitinos escape detection, the typical signature of these SUSY events is missing energy and isolated photons. Unless the contrary is explicitly stated, the Minimal Supersymmetric Standard Model (MSSM) scheme with universal parameters at the high mass scale typical of Grand Unified Theories (GUT's) is assumed [1]. The parameters of this model relevant to the present searches are the masses $M_1$ and $M_2$ of the gaugino sector (which are assumed to satisfy the GUT relation $M_1 = \frac{5}{3}\tan^2\theta_W M_2 \approx 0.5 M_2$ at the electroweak scale), the universal mass $m_0$ of the scalar lepton sector (which enters mainly via the sneutrino mass), the Higgs mass parameter $\mu$, and the ratio $\tan\beta$ of vacuum expectation values of the two Higgs doublets. In this scheme, the chargino production cross-section at a given energy can be greatly reduced by destructive interference between the $s$-channel and $t$-channel contributions if the sneutrino mass is below 300 $\mathrm{GeV}/c^2$ and the SUSY parameters take particular values [6].

# 2 Data samples and event generators

The total integrated luminosity collected by DELPHI during 1997 at $E_{cm} = 183$ GeV was 53.9 $\mathrm{pb}^{-1}$. This luminosity was used in the chargino analysis for topologies with a stable neutralino, while 50.6 $\mathrm{pb}^{-1}$ was used in topologies with an unstable neutralino due to a temporary problem in the read-out of the barrel electromagnetic calorimeter (HPC). The luminosity used in the neutralino analysis was 47.3 $\mathrm{pb}^{-1}$.

To evaluate the signal efficiencies and background contaminations, events were generated using several different programs. All relied on `JETSET` 7.4 [7], tuned to LEP 1 data [8], for quark fragmentation.

The program `SUSYGEN` [9] was used to generate neutralino and chargino signal events in both the neutralino LSP and the gravitino LSP scenarios, and to calculate cross-sections and branching ratios. These agree with the calculations of Ref. [10]. Details of the signal samples generated are given in section 4.

The background process $\mathrm{e^+e^-} \to \mathrm{q\bar{q}}(n\gamma)$ was generated with `PYTHIA 5.7` [7], while

DYMU3 [11] and KORALZ [12] were used for $\mu^+\mu^-(\gamma)$ and $\tau^+\tau^-(\gamma)$, respectively. The generator of Ref. [13] was used for $e^+e^- \to e^+e^-$ events. Processes leading to four-fermion final states, $(Z/\gamma)^*(Z/\gamma)^*$, $W^+W^-$, $We\nu_e$ and $Ze^+e^-$, were also generated using PYTHIA. The calculation of the four-fermion background was verified using the program EXCALIBUR [14], which consistently takes into account all amplitudes leading to a given four-fermion final state. EXCALIBUR does not, however, include the transverse momentum of initial state radiation in the case where electrons are present in the final state.

Two-photon interactions leading to hadronic final states were generated using TWOGAM [15], separating the VDM, and QCD components. The generators of Berends, Daverveldt and Kleiss [16] were used for the QPM component and for leptonic final states.

The generated signal and background events were passed through the detailed simulation of the DELPHI detector [17] and then processed with the same reconstruction and analysis programs as the real data. The simulated number of events from different background processes was several times the number in the real data.

# 3 Event selections

The criteria used to select events were defined on the basis of the simulated signal and background events. The selections for charged and neutral particles were similar to those presented in [2], requiring charged particles to have momentum above 100 MeV/$c$ and to extrapolate back to within 5 cm of the main vertex in the transverse plane, and to within twice this distance in the longitudinal direction. Calorimeter energy clusters above 100 MeV were taken as neutral particles if not associated to any charged particle track. The particle selection was followed by different event selections for the different signal topologies as described in [2]. Fig. 1 shows the distribution of variables relevant for the selection of chargino topologies with a stable neutralino, for real and simulated events. The agreement is good; the normalisation is absolute.

The description of the differences in the selection criteria between the present analysis and the one at $\sqrt{s}$ = 161,172 GeV [2] follows here.

## 3.1 Chargino analysis

For the $jj\ell$ topology, in the degenerate case ($\Delta M \leq 10$ GeV/$c^2$), the minimum missing transverse momentum was changed from 3 to 4 GeV/$c$ and a new requirement was introduced: both jet axes had to point in region of the polar angle $24^\circ < \theta < 156^\circ$.

For the *jets* topology, in the non-degenerate case ($\Delta M > 10$ GeV/$c^2$), the maximum allowed energy in the forward and backward 20° cones was changed from 30% of the visible energy to 50%, the maximum visible mass was changed to 65 GeV/$c^2$, and a new lower cut on the visible mass of 15 GeV/$c^2$ was added. The same cut as in the $jj\ell$ topology, on the polar angle of the jets, was added in the degenerate case.

For the leptonic topology the different multiplicity dependent criteria on the missing transverse momentum were changed to a single minimum value of 5.5 GeV/$c$ for the non-degenerate case and 4 GeV/$c$ for the degenerate case.

For the radiative topology, i.e. chargino decays into $\gamma\gamma$X final states, the requirement that the total visible mass should exceed 20 GeV/$c^2$ was added in the non-degenerate case. In the degenerate case (re-defined to be 5 GeV/$c^2$ $< \Delta M \leq 10$ GeV/$c^2$) the minimum

scaled acoplanarity was changed from 5° to 10° and the momentum of the most energetic charged particle was required to not exceed 15 GeV/$c$, rather than 30 GeV/$c$. A new ultra-degenerate selection was introduced to increase the signal efficiency for $\Delta M \leq 5$ GeV/$c^2$. In this case, the energy of the most energetic isolated photon had to lie between 20 GeV and 60 GeV, and the momentum of the most energetic charged particle was required to be smaller than 10 GeV/$c$. The visible mass of the event, excluding the isolated photons, had to be smaller than 40 GeV/$c^2$, and the scaled acoplanarity greater than 5°. Finally, criteria similar to those in the degenerate case were applied in the missing transverse momentum, in the percentage of energy in the forward and backward 25° cones and in the total electromagnetic energy, excluding the energy of the most energetic isolated photon.

## 3.2 Neutralino analysis

A new selection criterion on the charged multiplicity was added to select $jj$ topology: in order to select hadronic events, at least four well reconstructed charged particles, including one with a transverse momentum exceeding 1 GeV/$c$, were required. Other new selection criteria were added: the sum of the absolute value of the momentum of well reconstructed charged particles had to be greater than 4 GeV/$c$; the transverse energy of the event should be greater than 4 GeV; no charged track was allowed to have a momentum greater than 20 GeV/$c$; finally the most isolated loosely identified electron or muon, with an isolation angle to the nearest jet greater than 20°, was required to have a momentum less than 10 GeV/$c$. The maximum allowed fraction of total energy of particles emitted within 30° of the beam was changed from 40% to 60%. The minimum allowed missing transverse momentum was changed to 4 GeV/$c$.

For low $\Delta M$ ($\sim$ 10 GeV/$c^2$), in the hadronic topology a lower cut on the scaled acoplanarity [2] (40°) and on the missing transverse momentum (7.0 GeV/$c$) were added. For intermediate $\Delta M$ ($\sim$ 40 GeV/$c^2$) the selection criteria on the multiplicity, on the total energy in the forward and backward 30° cone, and on the polar angle of missing momentum were removed. The allowed visible mass value was changed to be greater than 0.1 and less than $0.3\sqrt{s}/c^2$, the minimum missing mass value was changed from $0.5\sqrt{s}/c^2$ to $0.6\sqrt{s}/c^2$. For large $\Delta M$ ($\sim$ 90 GeV/$c^2$) all selection criteria are new: the invariant mass of visible particles was required to be greater than 0.3 and less than $0.5\sqrt{s}/c^2$, and the missing mass had to exceed $0.45\sqrt{s}/c^2$. The scaled acoplanarity had to exceed 25° and the missing transverse momentum had to exceed 8 GeV/$c$ and be less than 35 GeV/$c$. It was also required that the missing momentum along the beam-pipe should be less than 35 GeV/$c$.

A new analysis has been performed to select neutralino decays giving $\ell\ell$ final states. To select the di-lepton topology, two and only two isolated, oppositely charged, particles were required with momenta above 1 GeV/$c$. For the two selected tracks it was also required that both should have been reconstructed with at least four pad rows in the TPC and at least one hit in the VD. Finally, either both particles had to be at least loosely identified as an electron or a muon according to [17], or one of the particles had to be identified as an electron with at least the *standard tag*. To reject $e^+e^- \to e^+e^-$ and $Z\gamma$ events, the acoplanarity between the two selected particles was required to exceed 10°. Events produced in two photon interactions were rejected by demanding that the absolute value of the cosine of the polar angle of the missing momentum was less than

0.9, and that the transverse missing momentum had to be greater than 5 GeV/$c$ . It was also required that the energy in the 30° cone around the beam had to be less than 70 % of the visible energy and that no more than 1 GeV energy was registered in the STIC. To reduce the number of events from leptonic decays of $W^+W^-$pairs, an event was rejected if one particle was loosely identified as an electron and the other as a muon. In a similar manner as in the $jj$ topology the last step in the selection consisted of three sets of cuts, optimised for different regions of $\Delta M$.

- Low $\Delta M$ ($\sim$ 10 GeV/$c^2$): the invariant mass of visible particles was required to be less than $0.1\sqrt{s}/c^2$, the missing mass had to exceed $0.7\sqrt{s}/c^2$, the acoplanarity had to exceed 40° and missing transverse momentum had to exceed 8.0 GeV/$c$.
- Intermediate $\Delta M$ ($\sim$ 40 GeV/$c^2$): the invariant mass of visible particles was required to be greater than 0.1 and less than $0.3\sqrt{s}/c^2$, and the missing mass had to exceed $0.45\sqrt{s}/c^2$. The acoplanarity had to exceed 25° and missing transverse momentum had to exceed 10 GeV/$c$.
- Large $\Delta M$ ($\sim$ 90 GeV/$c^2$): the invariant mass of visible particles was required to be greater than 0.3 and less than $0.55\sqrt{s}/c^2$, and the missing mass had to exceed $0.4\sqrt{s}/c^2$. The acoplanarity had to exceed 15° and the missing transverse momentum had to exceed 12 GeV/$c$.

# 4 Results in case of a stable neutralino

## 4.1 Efficiencies and selected events

The total number of background events expected in the different topologies is shown in tables 1 and 2, together with the number of events selected in the data.

| | Chargino channels (stable neutralino) | | | | | |
|---|---|---|---|---|---|---|
| | Non-degenerate selection | | | Degenerate selection | | |
| Topology: | $jj\ell$ | *jets* | $\ell\ell$ | $jj\ell$ | *jets* | $\ell\ell$ |
| Obs. events: | 0 | 11 | 7 | 4 | 3 | 1 |
| Background: | 1.0 ± 0.8 | 7.6 ± 0.9 | 8.8 ± 1.0 | 3.3 ± 0.9 | 5.1 ± 0.9 | 1.9 ± 0.8 |
| Total: | | | | | | |
| Obs. events: | 18 | | | 8 | | |
| Background: | 17.4 ± 1.1 | | | 10.3 ± 1.1 | | |

Table 1: The number of events observed in data and the expected number of background events in the different chargino search channels under the hypothesis of a stable neutralino (section 3.1).

The efficiencies of the chargino selections in section 3.1 were estimated using 37 combinations of $\tilde{\chi}_1^\pm$ and $\tilde{\chi}_1^0$ masses in four chargino mass ranges ($M_{\tilde{\chi}_1^\pm} \approx$ 91, 85, 70 and 50 GeV/$c^2$) and with $\Delta M$ ranging from 1 GeV/$c^2$ to 70 GeV/$c^2$. A total of 74000

| | Neutralino channels | |
|---|---|---|
| Topology: | $jj$ | $\ell\ell$ |
| Obs. events: | 6 | 5 |
| Background: | 8.2 ± 1.2 | 6.9 ± 0.6 |

Table 2: The number of events observed in data and the expected number of background events in the different neutralino search channels (sections 3.2).

chargino events was generated and passed through the complete simulation of the DELPHI detector. A special study was carried out in the region of low $|\mu|$ and $M_2$ as already described in [2]. The efficiencies for the four different topologies are shown in Fig. 2.

For the neutralino analysis, a total of 130000 $\tilde{\chi}^0_1\tilde{\chi}^0_2$ events was generated for 42 different combinations of $M_{\tilde{\chi}^0_2}$ and $M_{\tilde{\chi}^0_1}$ masses with $M_{\tilde{\chi}^0_1}$ ranging from 10 GeV/$c^2$ to 85 GeV/$c^2$, with $M_{\tilde{\chi}^0_2} - M_{\tilde{\chi}^0_1}$ ranging from 5 GeV/$c^2$ to the kinematic limit, and for different $\tilde{\chi}^0_2$ decay modes ($\mathrm{q\bar{q}}\tilde{\chi}^0_1$, $\mu^+\mu^-\tilde{\chi}^0_1$, $\mathrm{e^+e^-}\tilde{\chi}^0_1$). The efficiencies for the neutralino selections in section 3.2 are shown in Fig. 3.

All the selected events are compatible with the expectation from the bacground simulation. As no evidence for a signal is found, exclusion limits are set.

### 4.1.1 Limits

*Limits on chargino production*

The simulated data points were used to parametrise the efficiencies of the chargino selection criteria described in section 3.1 in terms of $\Delta M$ and the mass of the chargino. Then a large number of SUSY points were investigated and the values of $\Delta M$, the chargino and neutralino masses and the various decay branching ratios were determined for each point. By applying the appropriate efficiency and branching ratios for each channel the number of expected signal events for a given cross-section can be calculated. Taking also the expected background and the number of events actually observed into account, certain cross sections, or the corresponding points in the MSSM parameter space ($\mu$, $M_2$, $\tan\beta$), may be excluded.

Fig. 4 shows the chargino production cross-sections as obtained in the MSSM at $\sqrt{s}$ = 183 GeV for different chargino masses for the non-degenerate and degenerate cases. The parameters $M_2$ and $\mu$ were varied randomly in the ranges 0 GeV/$c^2$ < $M_2$ < 3000 GeV/$c^2$ and –400 GeV/$c^2$ < $\mu$ < 400 GeV/$c^2$ for three different values of $\tan\beta$, namely 1, 1.5 and 35. Two different cases were considered for the sneutrino mass: $M_{\tilde{\nu}} > 300$ GeV/$c^2$ (in the non degenerate case) and $M_{\tilde{\nu}} > 41$ GeV/$c^2$ (in the degenerate case).

Applying the appropriate efficiencies and branching ratios for each of the points shown the minimum non-excluded $M_{\tilde{\chi}^\pm_1}$ was determined.

To derive the chargino mass limits, constraints on the process $\mathrm{Z} \to \tilde{\chi}^0_1\tilde{\chi}^0_2 \to \tilde{\chi}^0_1\tilde{\chi}^0_1\gamma$ were also included. These were derived from the DELPHI results on single-photon production at LEP 1 [18].

The chargino mass limits are summarized in Table 3. The table also gives, for each

case, the minimum excluded MSSM cross-section provided that $M_{\tilde{\chi}_1^\pm}$ is below the appropriate mass limit. These cross-section values are also displayed in Fig. 4.

The excluded region in the plane of neutralino mass versus chargino mass, assuming a heavy sneutrino, is shown in Fig. 5.

In the non-degenerate case with a large sneutrino mass ($> 300$ GeV/$c^2$), the lower limit for the chargino ranges between 89.4 GeV/$c^2$ (for a mostly higgsino-like chargino) and 90.8 GeV/$c^2$ (for a mostly wino-like chargino). The minimum excluded MSSM cross-section at $\sqrt{s} = 183$ GeV is 0.82 pb, provided that $M_{\tilde{\chi}_1^\pm}$ is below 89.4 GeV/$c^2$.

In the degenerate case ($\Delta M = 5$ GeV/$c^2$), the cross-section does not depend significantly on the sneutrino mass, since the chargino is higgsino-like under the assumption of gaugino mass unification. The lower limit for the chargino mass, shown in Fig. 4, is 88.8 GeV/$c^2$. The lower cross section limit is in this case 0.95 pb.

| **Case** | $m_{\tilde{\nu}}$ (GeV/$c^2$) | $M_{\chi^\pm}^{min}$ (GeV/$c^2$) | $\sigma^{max}$ (pb) | $N_{95\%}$ |
|---|---|---|---|---|
| Stable neutralino | | | | |
| $\Delta M > 10$ GeV/$c^2$ | $> 300$ | 89.4 | 0.82 | 10.14 |
| $\Delta M = 5$ GeV/$c^2$ | $> 41$ | 88.8 | 0.95 | 6.39 |
| Unstable neutralino | | | | |
| $\Delta M > 10$ GeV/$c^2$ | $> 300$ | 90.5 | 0.49 | 4.69 |
| $\Delta M = 1$ GeV/$c^2$ | $> 41$ | 90.6 | 0.45 | 4.36 |

Table 3: 95% confidence level limits for the chargino mass, the corresponding pair production cross-sections at 183 GeV and the 95% confidence level upper limit on number of observed events, for the non-degenerate and a highly degenerate cases. The scenarios of a stable $\tilde{\chi}_1^0$ and $\tilde{\chi}_1^0 \to \tilde{G}\gamma$ are considered.

*Limits on neutralino production*

Limits on neutralino production in the case of a stable $\tilde{\chi}_1^0$ were derived from the parametrised efficiencies of section 3.2 and the observed number of events, in the same way as it is described in [2]. The limits obtained for the $\tilde{\chi}_1^0\tilde{\chi}_2^0$ production cross-section are shown in Figs. 6a,b and c assuming hadronic or leptonic decay modes. The limit

obtained assuming that the $\tilde{\chi}_2^0 \to \tilde{\chi}_1^0 f\bar{f}$ decay is mediated by a $Z^*$, including both leptonic and hadronic modes and 20% of invisible final states, is presented in Fig. 6d. These limits also apply to $\tilde{\chi}_1^0\tilde{\chi}_k^0$ ($k$=3,4) production with $\tilde{\chi}_k^0$ decaying into $\tilde{\chi}_1^0$.

*Limits on MSSM parameters and neutralino mass*

The result of the searches for charginos and neutralinos in the different topologies for a stable neutralino can be interpreted in the MSSM with a universal GUT scale gaugino mass parameter. This yields the exclusion regions in the $(\mu, M_2)$ plane shown in Fig. 7 for different values of $\tan\beta$, assuming a heavy sneutrino and a heavy selectron ($m_0$ = 1 TeV/$c^2$). When different event selections contributed to the same physical production channel the efficiency and background of a logical OR of the channels was used, otherwise the method of Ref. [19] was used to combine the selections. These limits, based on data taken at $\sqrt{s}$ =183 GeV, improve on previous limits at lower energies, and represent a significant increase in range as compared to LEP 1 results [20]. The neutralino analysis independently excludes a substantial part of the region covered by the chargino search, and marginally extends this region for low $\tan\beta$.

Note that the neutralino masses, and hence the regions in the ($\mu$,$M_2$) plane excluded by the neutralino search, depend directly on the assumed GUT relation $M_1/M_2 = \frac{5}{3}\tan^2\theta_W \approx 0.5$. The region excluded by the chargino search on the other hand depends on this ratio only via the effect of decay kinematics on the efficiency. While the $M_{\tilde{\chi}_1^0}+M_{\tilde{\chi}_2^0}$ isomass contours relevant to the present neutralino search depend only weakly on this ratio, any consideration about the minimum $M_{\tilde{\chi}_1^0}$ that can be excluded depends sensitively on the relation between $M_1$ and $M_2$.

Under the assumption that $M_1/M_2 \gtrsim 0.5$, the exclusion regions in the ($\mu$,$M_2$) plane can be translated into a limit on the mass of the lightest neutralino. A lower limit of 29.1 GeV/$c^2$ on the lighest neutralino mass is then obtained, valid for $\tan\beta \geq 1$, using the obtained chargino exclusion regions and including the DELPHI results [18] on the process $Z \to \tilde{\chi}_1^0\tilde{\chi}_2^0 \to \tilde{\chi}_1^0\tilde{\chi}_1^0\gamma$ . The lower mass limit is obtained for $\tan\beta = 1$, $\mu$ = -62.3 GeV/$c^2$, $M_2$ = 46.0 GeV/$c^2$. Fig. 8 shows the limit on $M_{\tilde{\chi}_1^0}$ as a function of $\tan\beta$.

## 4.2 Results in case of an unstable neutralino

### 4.2.1 Efficiencies and selected events

The efficiency of the chargino selection for an unstable neutralino decaying into a photon and a gravitino was calculated from a total of 78000 events generated using the same combinations of $M_{\tilde{\chi}_1^\pm}$ and $M_{\tilde{\chi}_1^0}$ as in the stable neutralino scenario. As mentioned in [2], the same selection applies to all topologies. The efficiency, as shown in Fig. 9, varies only weakly with $\Delta M$ and is around 50%. Note that, due to the presence of the photons from the neutralino decay, the region of high degeneracy (down to $\Delta M$ = 1 GeV/$c^2$) is fully covered.

The total number of background events expected in the different $\Delta M$ ranges is shown in table 4, together with the number of events selected in the data. 4 events were found in the data, with a total expected background of 6.3±0.9. No signal is found, exclusion limits are set.

| | Chargino channels (unstable neutralino) | | |
|---|---|---|---|
| | Non-degenerate selection | Degenerate selection | Ultra-degenerate selection |
| Obs. events: | 3 | 0 | 1 |
| Background: | $4.9 \pm 0.8$ | $0.9 \pm 0.3$ | $0.5 \pm 0.2$ |

Table 4: The number of events observed and the expected number of background events in the different $\Delta M$ cases under the hypothesis of an unstable neutralino (section 3.1).

### 4.2.2 Limits

The chargino cross-section limits corresponding to the case where the neutralino is unstable and decays via $\tilde{\chi}_1^0 \to \tilde{\mathrm{G}}\gamma$ are computed as explained in section 4.1.1 and they are shown in Fig.10, and in table 3. In the non-degenerate case the chargino mass limit at 95% confidence level is 90.5 GeV/$c^2$ for a heavy sneutrino, while in the ultra-degenerate case ($\Delta M = 1$ GeV/$c^2$) the limit is 90.6 GeV/$c^2$. The minimum MSSM cross-section excluded by the above mass limits are 0.49 pb in the non degenerate case and 0.45 pb in the ultra-degenerate case.

# 5 Summary

Searches for charginos and neutralinos at $\sqrt{s} = 183$ GeV allow the exclusion of a large domain of SUSY parameters.

Assuming a difference in mass between chargino and neutralino, $\Delta M$, of 10 GeV/$c^2$ or more, and a sneutrino heavier than 300 GeV/$c^2$, the existence of a chargino lighter than 89.4 GeV/$c^2$ can be excluded. If a gaugino-dominated chargino is assumed in addition, the kinematic limit is reached. If $\Delta M$ is between 5 GeV/$c^2$ and 10 GeV/$c^2$, the lower limit on the chargino mass becomes 88.8 GeV/$c^2$, independent of the sneutrino mass.

Limits on the cross-section for $\tilde{\chi}_1^0\tilde{\chi}_2^0$ production of about 1 pb are obtained, and the excluded region in the ($\mu$,$M_2$) plane is extended by the combined use of the neutralino and chargino searches. A special study of the low $|\mu|$, $M_2$, $\tan\beta$ region gives a limit on the mass of the lightest neutralino, valid in the case of large $m_0$, of 29.1 GeV/$c^2$ at 95% confidence level.

A specific $\tilde{\chi}_1^+\tilde{\chi}_1^-$ production search was performed assuming the decay of the lightest neutralino into photon and gravitino, giving somewhat more stringent limits on cross-sections and masses than in the case of a stable $\tilde{\chi}_1^0$.

# Acknowledgements

We are greatly indebted to our technical collaborators and to the funding agencies for their support in building and operating the DELPHI detector. We also want to thank the members of the CERN accelerator divisons for the continued excellent performance of the LEP collider in the energy range above the Z resonance.

# References


[1] P. Fayet and S. Ferrara, Phys. Rep. **32** (1977) 249;
H.P. Nilles, Phys. Rep. **110** (1984) 1;
H.E. Haber and G.L. Kane, Phys. Rep. **117** (1985) 75.

[2] DELPHI Coll., P. Abreu *et al.*, Eur. Phys. J. **C1** (1998) 1-20.

[3] D. Dicus *et al.*, Phys. Rev. **D41** (1990) 2347;
D. Dicus *et al.*, Phys. Rev. **D43** (1991) 2951;
D. Dicus *et al.*, Phys. Lett. **B258** (1991) 231.

[4] S. Dimopoulos *et al.*, Phys. Rev. Lett. **76** (1996) 3494;
S. Ambrosanio *et al.*, Phys. Rev. Lett. **76** (1996) 3498;
J.L. Lopez and D.V. Nanopoulos, Mod. Phys. Lett. **A10** (1996) 2473;
J.L. Lopez and D.V. Nanopoulos, Phys. Rev. **D55** (1997) 4450.

[5] S. Ambrosanio *et al.*, Phys. Rev. **D54** (1996) 5395.

[6] A.Bartl, H.Fraas and W. Majerotto, Z. Phys. **C30** (1986) 441;
A.Bartl, H.Fraas and W. Majerotto, Z. Phys. **C41** (1988) 475;
A.Bartl, H.Fraas, W. Majerotto and B.Mösslacher, Z. Phys. **C55** (1992) 257.

[7] T. Sjöstrand, Comp. Phys. Comm. **39** (1986) 347;
T. Sjöstrand, `PYTHIA 5.6` *and* `JETSET 7.3`, CERN-TH/6488-92.

[8] DELPHI Coll., P. Abreu *et al.*, Z. Phys. **C73** (1996) 11.

[9] S. Katsanevas and S. Melachroinos in *Physics at LEP2*, CERN 96-01, Vol. 2, p. 328.

[10] S. Ambrosanio and B. Mele, Phys. Rev. **D52** (1995) 3900;
S. Ambrosanio and B. Mele, Phys. Rev. **D53** (1996) 2451.

[11] J.E. Campagne and R. Zitoun, Z. Phys. **C43** (1989) 469.

[12] S. Jadach and Z. Was, Comp. Phys. Comm. **79** (1994) 503.

[13] F.A. Berends, R. Kleiss, W. Hollik, Nucl. Phys. **B304** (1988) 712.

[14] F.A. Berends, R. Pittau, R. Kleiss, Comp. Phys. Comm. **85** (1995) 437.

[15] S. Nova, A. Olshevski, and T. Todorov, *A Monte Carlo event generator for two photon physics*, DELPHI note 90-35 (1990).

[16] F.A. Berends, P.H. Daverveldt, R. Kleiss, Comp. Phys. Comm. **40** (1986) 271, Comp. Phys. Comm. **40** (1986) 285, Comp. Phys. Comm. **40** (1986) 309.

[17] DELPHI Coll., P. Aarnio *et al.*, Nucl. Instr. and Meth. **303** (1991) 233;
DELPHI Coll., P. Abreu *et al.*, Nucl. Instr. and Meth. **378** (1996) 57.

[18] DELPHI Coll., P. Abreu *et al.*, Z. Phys. **C74** (1997) 577

[19] V.F. Obraztsov, Nucl. Instr. and Meth. **316** (1992) 388.

[20] ALEPH Coll., D. Decamp *et al.*, Phys. Rep. **216** (1992) 253;
A. Lopez-Fernandez, DELPHI note 92-95 (Dallas) PHYS 206;
L3 Coll., M. Acciarri *et al.*, Phys. Lett. **B350** (1995) 109;
OPAL Coll., G. Alexander *et al.*, Phys. Lett. **B377** (1996) 273.

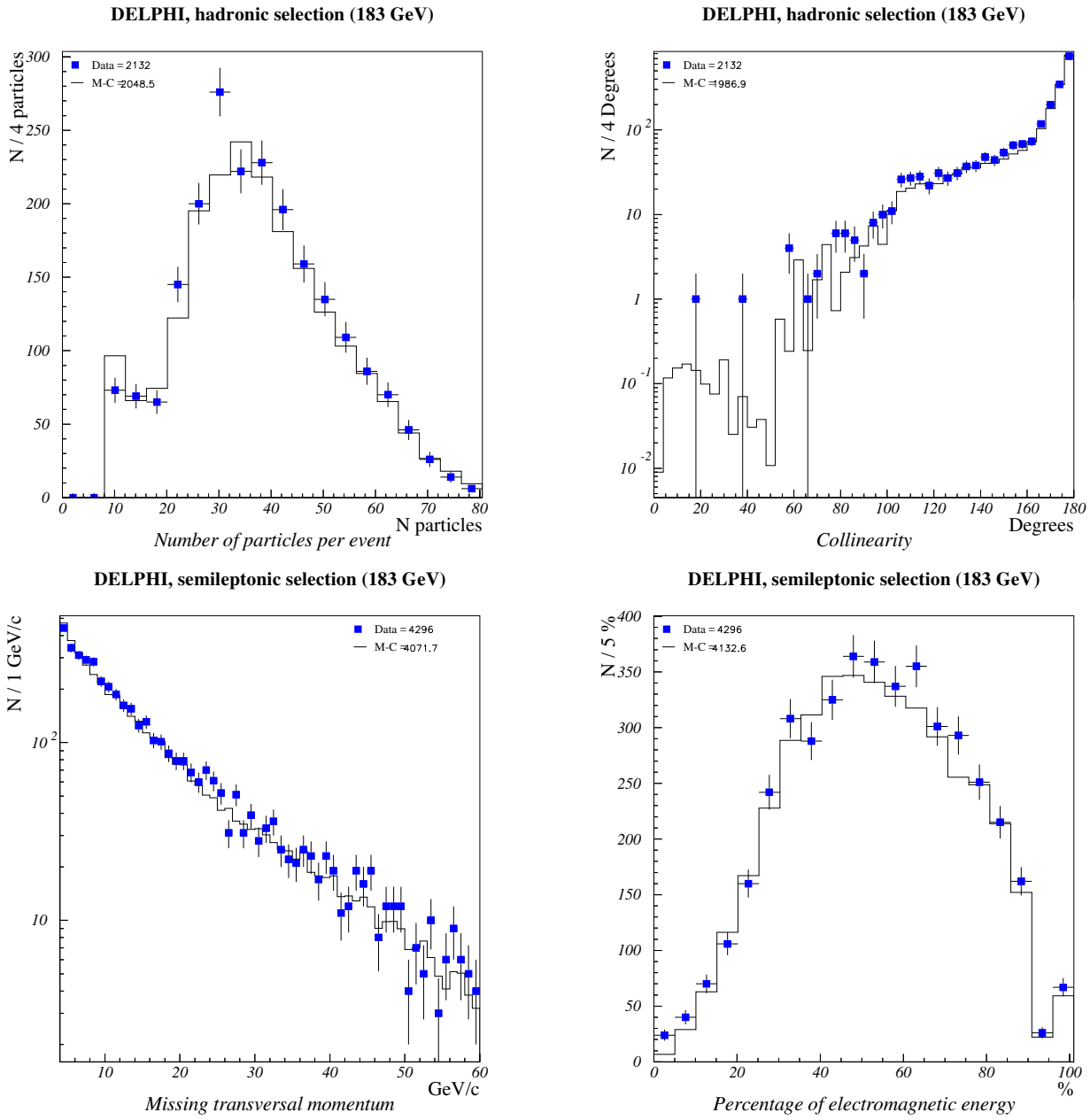


Figure 1: Distributions of total multiplicity and collinearity after hadronic preselection. Distributions of missing transversal momentum and percentage of electromagnetic energy after the semileptonic preselection. *Points* show distributions for real data events, *histograms* for simulated events. The hadronic preselection requires in addition to the event preselection criteria described in [2] that the missing transversal momentum is greater than 4 GeV/$c$, the percentage of energy in the forward and backward 20° cones is less than 50%, the polar angle of the leading neutral particle is between 11° and 169°. The semileptonic preselection requires in addition to the hadronic one the presence of an isolated lepton and a missing momentum with a polar angle between 30° and 150°.

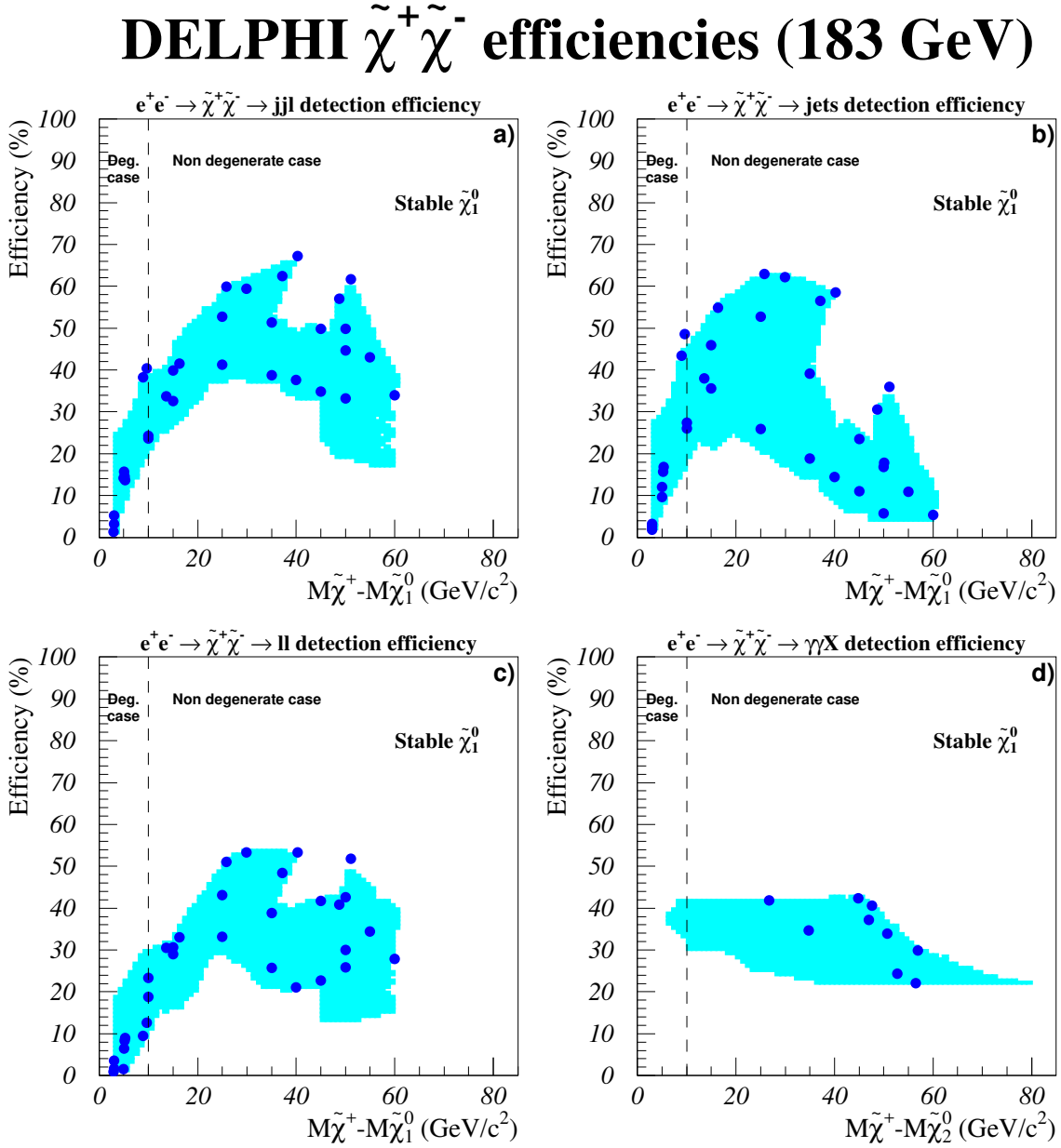


Figure 2: Chargino detection efficiencies (stable neutralino) for the 4 topologies a) $jj\ell$, b) *jets*, c) $\ell\ell$ and d) $\gamma\gamma$X, obtained combining four sets of selection criteria (section 3.1). Full circles are the efficiencies for the 37 fully simulated chargino points, the light gray area is the result of the parametrisation.

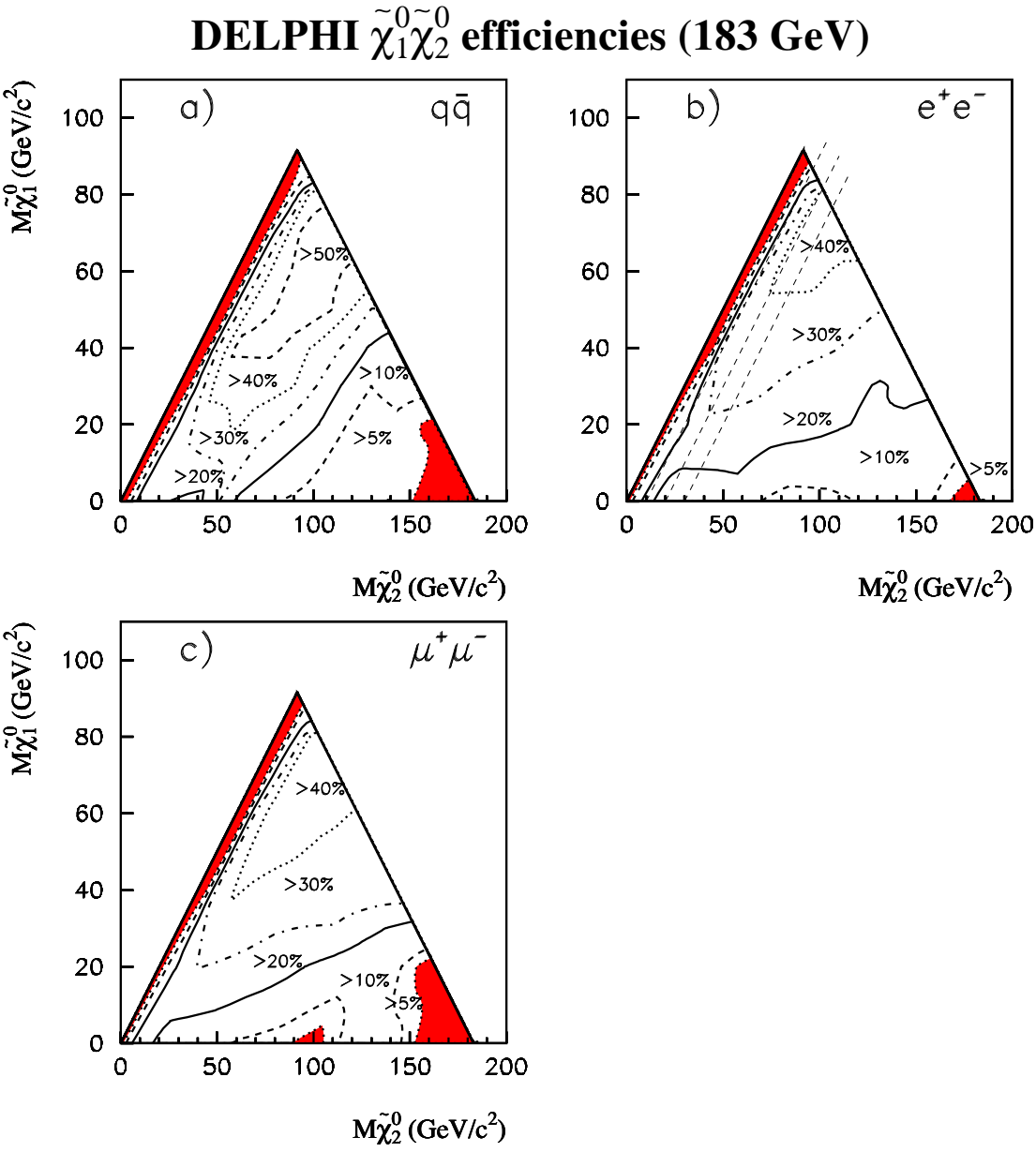


Figure 3: Neutralino pair production detection efficiency for the $jj$, $e^+e^-$ and $\mu^+\mu^-$ topologies at 183 GeV in the $(M_{\tilde{\chi}^0_2}, M_{\tilde{\chi}^0_1})$ plane.

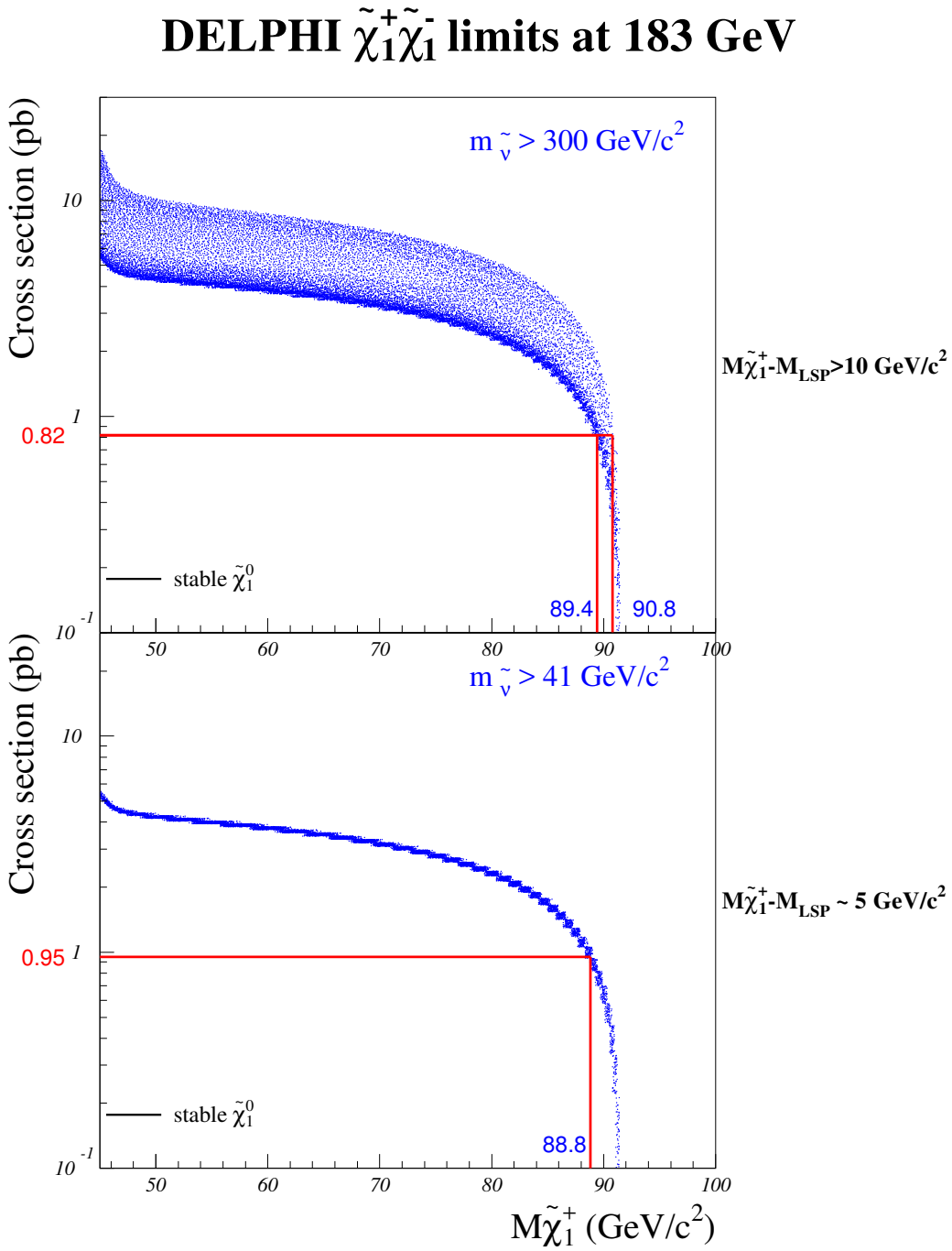


Figure 4: Expected cross-sections at 183 GeV (dots) versus the chargino mass in the non-degenerate scenario ($\Delta M > 10$ GeV/$c^2$) and in the degenerate scenario ($\Delta M \sim 5$ GeV/$c^2$), for different MSSM parameter values, in the case of stable neutralino. A heavy sneutrino ($m_{\tilde{\nu}} > 300$ GeV/$c^2$) has been assumed in the upper plot and $m_{\tilde{\nu}} > 41$ GeV/$c^2$ in the lower one. The cross-sections indicated are the minimum ones in the excluded mass region.

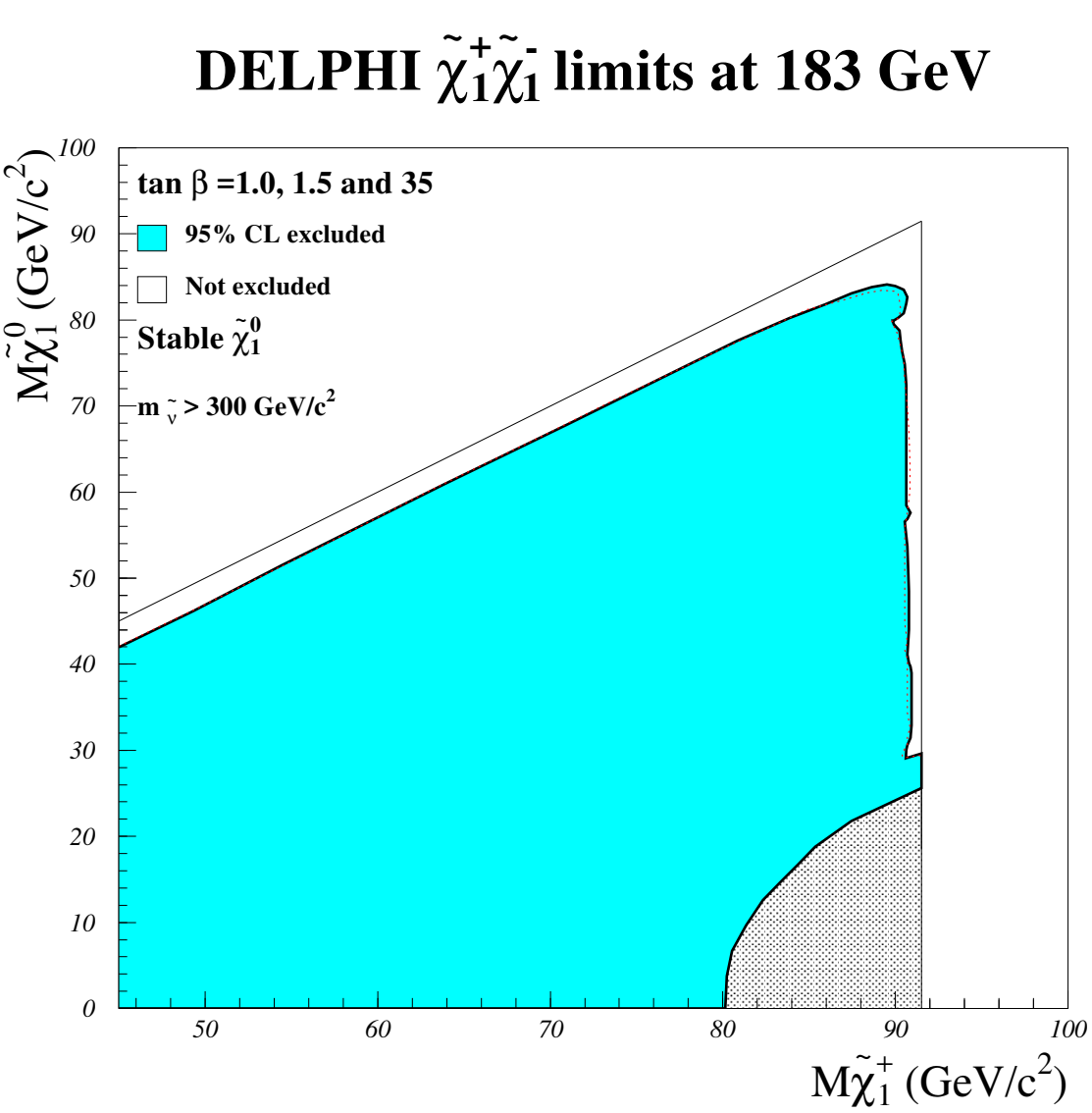


Figure 5: Regions excluded at 95% confidence level in the plane of the mass of the lightest neutralino versus that of the lightest chargino under the assumption of a heavy sneutrino. The thin lines show the kinematic limits in the production and the decay. The dotted line shows the expected exclusion limit. The lightly shaded region is not allowed in the MSSM. The limit applies in the case of a stable neutralino.

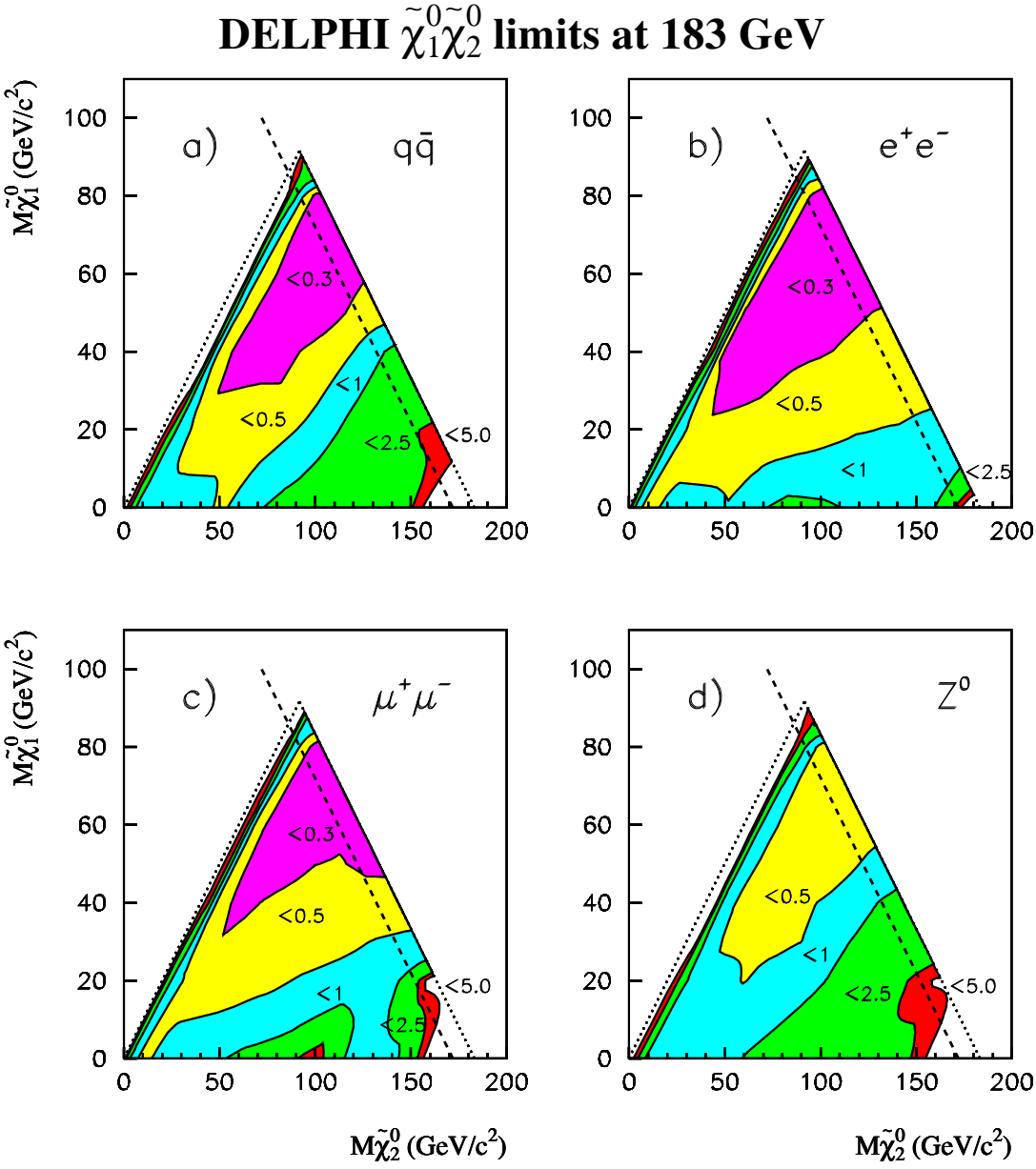


Figure 6: Contour plots of upper limits on the cross-sections at the 95% confidence level for $\tilde{\chi}^0_1\tilde{\chi}^0_2$ production at $\sqrt{s} = 183$ GeV. In each plot, the different shades correspond to regions where the cross-section limit in picobarns is below the indicated number. For figures a), b), c), $\tilde{\chi}^0_2$ decays into $\tilde{\chi}^0_1 q\bar{q}$, $\tilde{\chi}^0_1 e^+e^-$, and $\tilde{\chi}^0_1\mu^+\mu^-$, respectively, were assumed to dominate. In d), the $\tilde{\chi}^0_2$ was assumed to decay into $\tilde{\chi}^0_1 f\bar{f}$ with the same branching ratios into different fermion flavours as the Z. The dotted lines indicate the kinematic limit and the defining relation $M_{\tilde{\chi}^0_2} > M_{\tilde{\chi}^0_1}$.

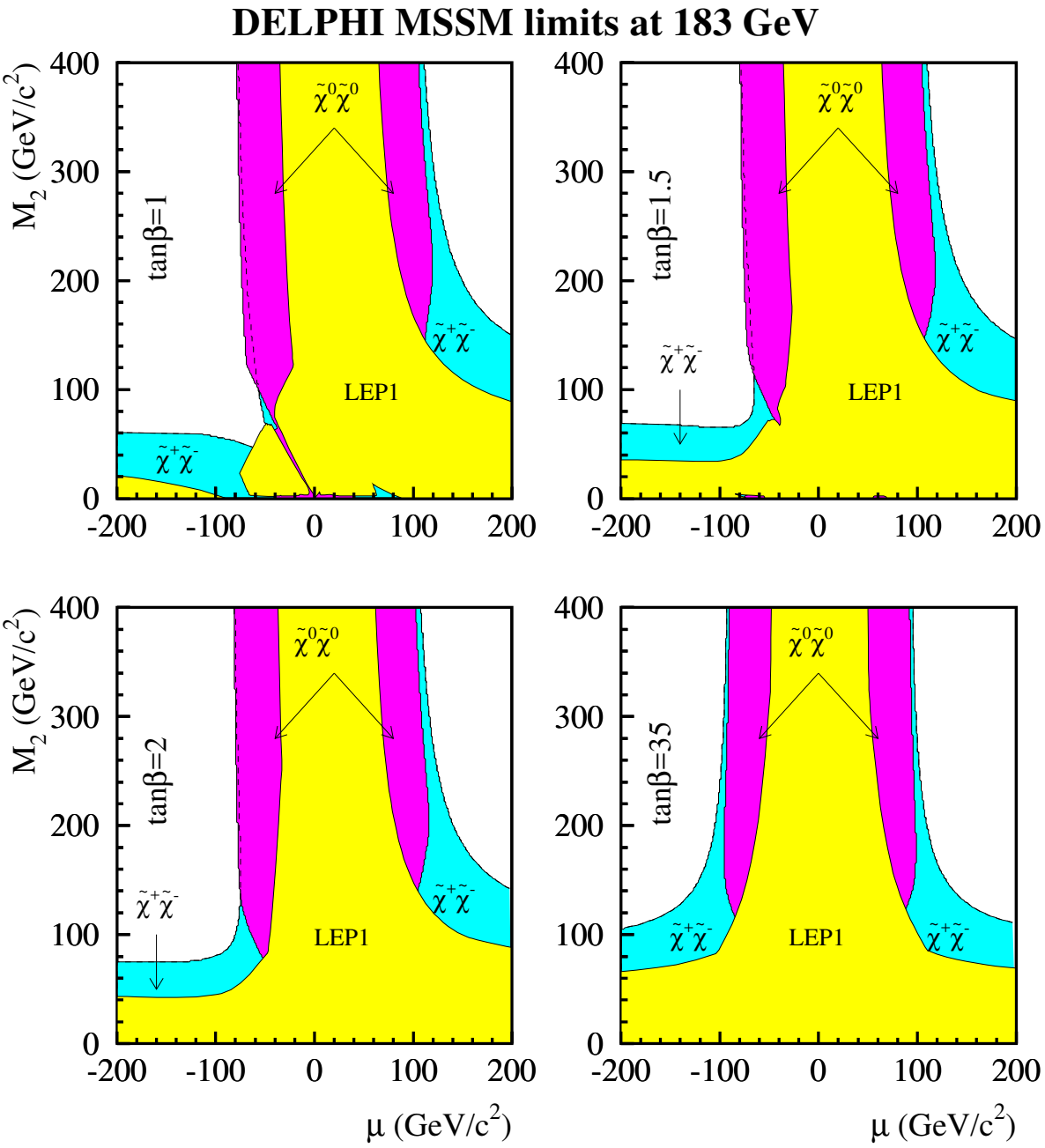


Figure 7: Regions in the $(\mu, M_2)$ plane excluded at 95% confidence level for different values of $\tan\beta$, assuming $m_0 = 1$ TeV/$c^2$. The lightly shaded areas are those excluded by lower energy LEP 1 results [20]. The intermediate shading shows regions excluded by the chargino search at 183 GeV. The darkly shaded areas show the regions excluded by the neutralino search at these energies. With the exception of a narrow strip at negative $\mu$ for $\tan\beta = 1$, indicated in black, the regions excluded by the neutralino results are also excluded by the chargino search.

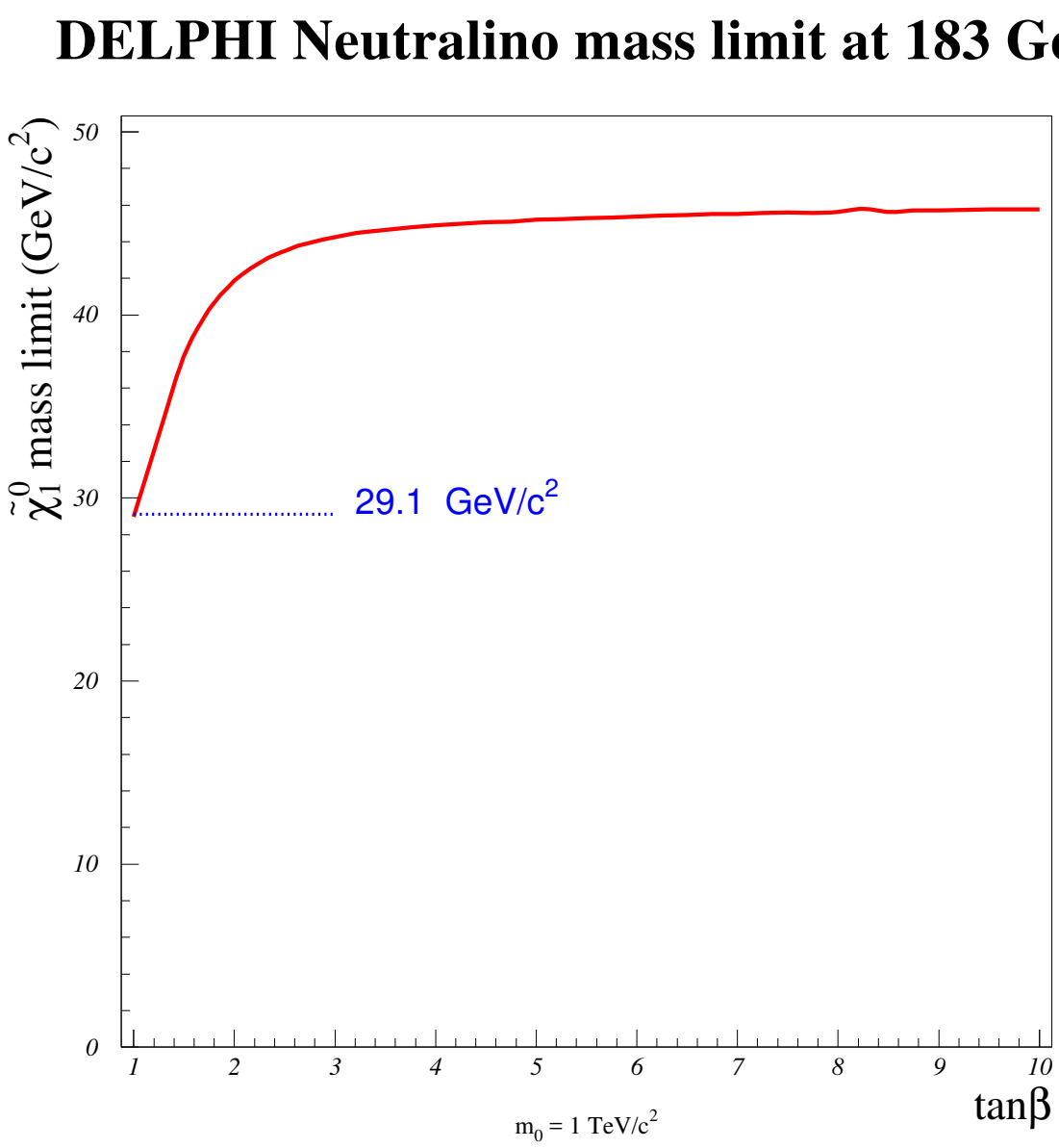


Figure 8: Lower limit at 95% confidence level on the mass of the lightest neutralino, $\tilde{\chi}_1^0$. as a function of $\tan\beta$ assuming a stable $\tilde{\chi}_1^0$ and $m_0 = 1$ TeV/$c^2$. The limit is obtained using the present limit on $\tilde{\chi}_1^+\tilde{\chi}_1^-$ search and the limit obtained on $\tilde{\chi}_1^0\tilde{\chi}_2^0$ production at the Z resonance derived from the single-photon search.

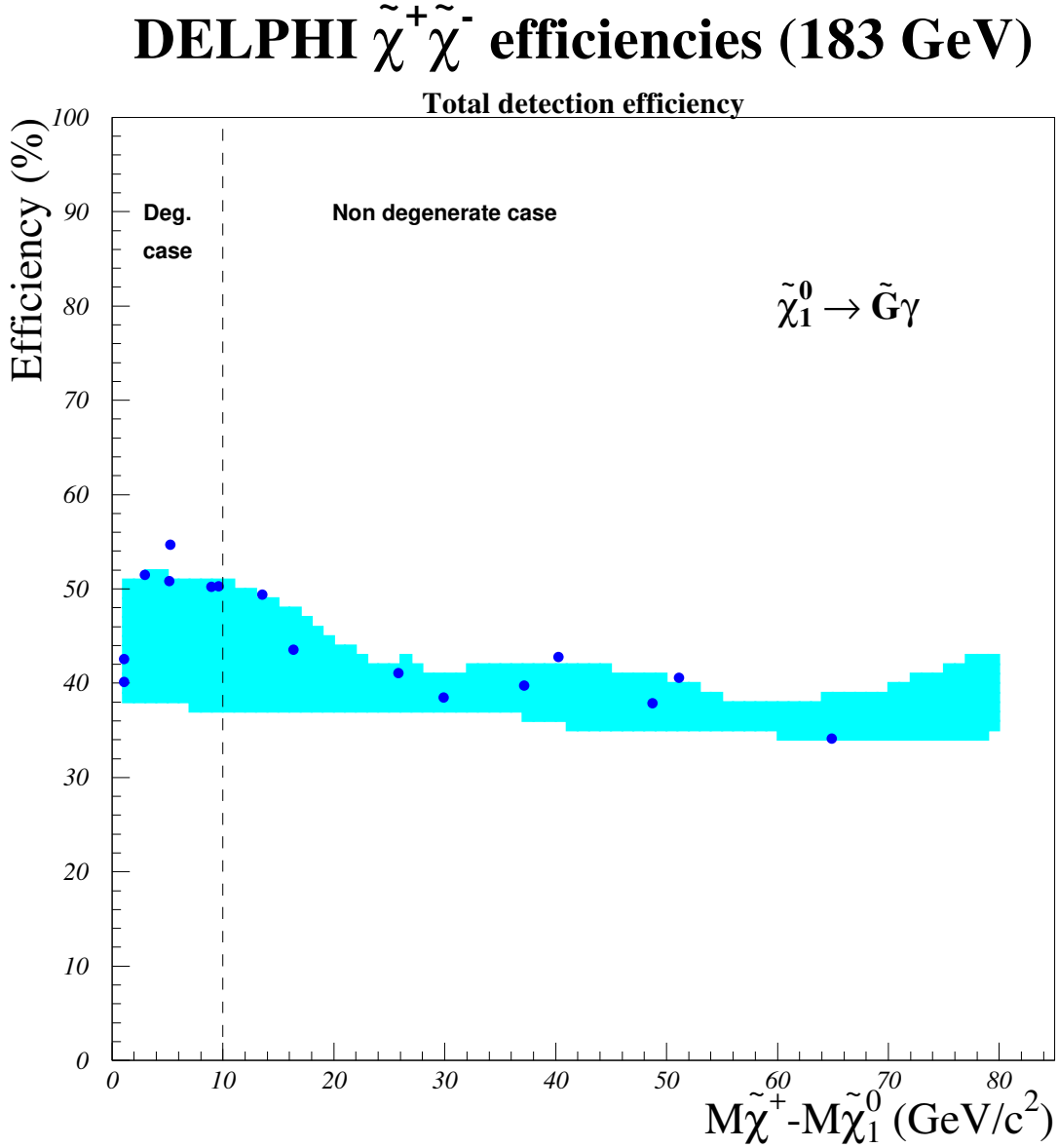


Figure 9: Chargino detection efficiencies in case on unstable neutralino. Full circles are the efficiencies for the 16 generated chargino points, the light gray area is the result of the parametrisation.

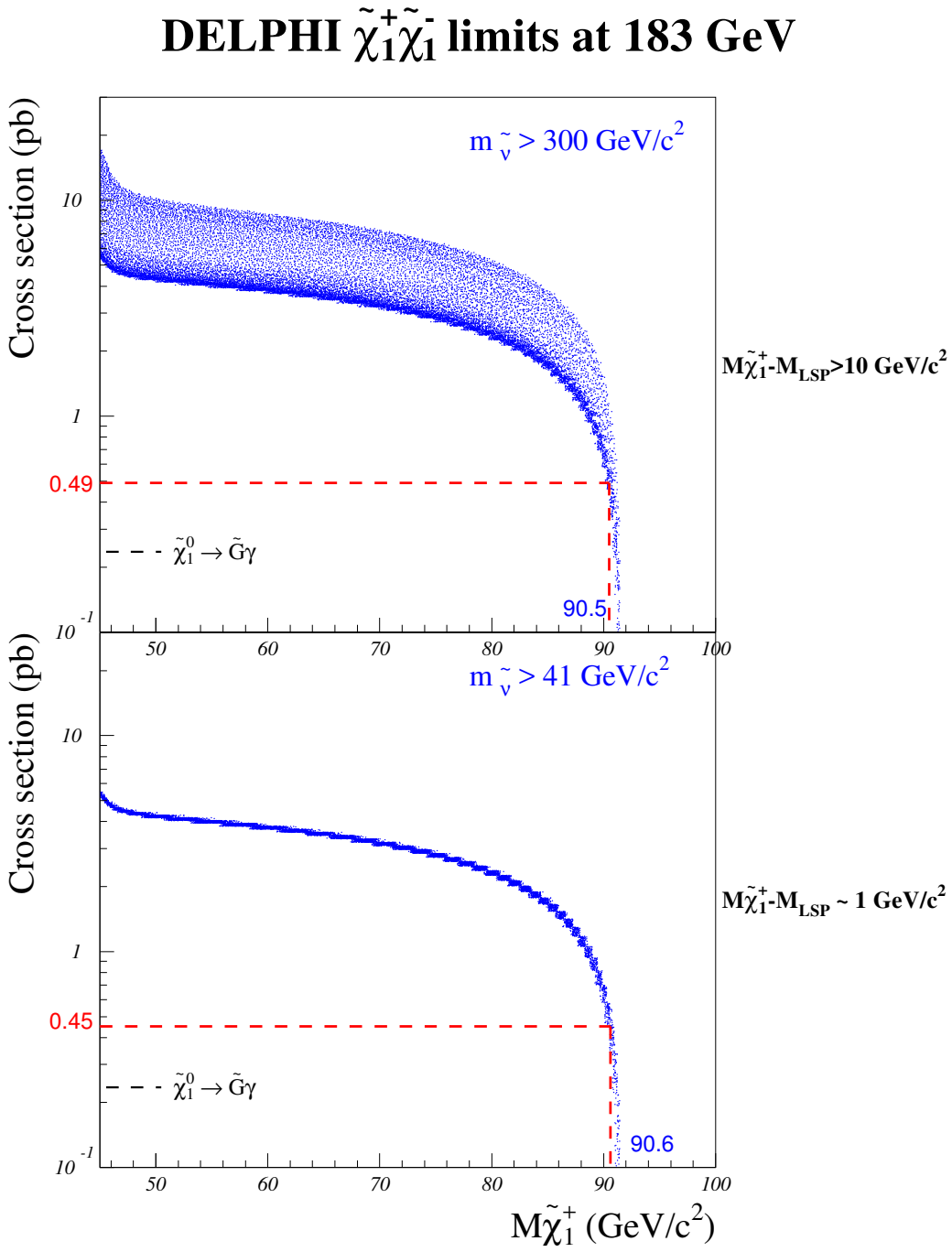


Figure 10: Expected cross-sections at 183 GeV (dots) versus the chargino mass in the non-degenerate scenario ($\Delta M >$ 10 GeV/$c^2$) and in the ultra-degenerate scenario ($\Delta M \sim$ 1 GeV/$c^2$), for different MSSM parameter values, in the case of unstable neutralino. A heavy sneutrino ($m_{\tilde{\nu}} >$ 300 GeV/$c^2$) has been assumed in the upper plot and $m_{\tilde{\nu}} >$ 41 GeV/$c^2$ in the lower one. The cross-sections indicated are the minimum ones in the excluded mass region.